

Rotating Shaft Tilt Angle Measurement Using an Inclinometer

Jun Luo^{1,2}, Zhiqian Wang¹, Chengwu Shen^{1,2}, Zhuoman Wen^{1,2}, Shaojin Liu¹, Chang Liu¹,
Sheng Cai¹, Jianrong Li¹

¹Changchun Institute of Optics, Fine Mechanics and Physics, Chinese Academy of Sciences,
Changchun 130033, China, wangzhiqian2000@gmail.com

²University of Chinese Academy of Sciences, Beijing 10049, China, luojun604@qq.com

This paper describes a novel measurement method to accurately measure the rotating shaft tilt angle of rotating machine for alignment or compensation using a dual-axis inclinometer. A model of the rotating shaft tilt angle measurement is established using a dual-axis inclinometer based on the designed mechanical structure, and the calculation equation between the rotating shaft tilt angle and the inclinometer axes outputs is derived under the condition that the inclinometer axes are perpendicular to the rotating shaft. The reversal measurement method is applied to decrease the effect of inclinometer drifts caused by temperature, to eliminate inclinometer and rotating shaft mechanical error and inclinometer systematic error to attain high measurement accuracy. The uncertainty estimation shows that the accuracy of rotating shaft tilt angle measurement depends mainly on the inclinometer uncertainty and its uncertainty is almost the same as the inclinometer uncertainty in the simulation. The experimental results indicate that measurement time is 4 seconds; the range of rotating shaft tilt angle is 0.002° and its standard deviation is 0.0006° using NS-5/P2 inclinometer, whose precision and resolution are $\pm 0.01^\circ$ and 0.0005° , respectively.

Keywords: Rotating shaft, tilt angle measurement, inclinometer, reversal measurement, uncertainty estimation.

1. INTRODUCTION

ROTATING shaft tilt angle measurement is vital for a large number of rotating instruments, including 3 dimensional profile rotary measuring system [1], 3 dimensional coordinate measurement system based on rotary-laser scanning [2] and north-finder. One prerequisite of achieving precise measurement results is that the rotating shafts of these instruments are aligned vertically. Take the north-finder which sets the initial orientation in targeting, pointing and inertial guidance, for instance, Prikhodko [3], Xie [4] and Arnaudov [5] adapted the multi-point measurement method to reduce the effect of gyroscope compass bias drift on azimuth measurements. They assumed the rotating shaft was perpendicular to the horizontal plane so that all measurements were performed in a local horizontal plane; however, in most cases, the angle between the rotating shaft and the horizontal plane does not equal to 90 degrees because of installation. In order to obtain precise measurement results, it is significant to measure the tilt angle between the real rotating shaft and the ideal one which is perpendicular to the horizontal plane.

Several methods have been used to study this topic; ranging from algorithm compensation to sensors measurement. Fang proposed a precision algorithm to compensate the alignment angle error between the gear axis and the vertical axis of gear measuring machines. This method significantly improved its measuring accuracy, but can only be applied on gear measuring machines [6]. Autocollimator for small angle measurement was used to measure deviation angle of various objects. It sent laser beams from laser unit and projected them to the reflector located on the shaft, then the reflected beams were received by photoelectric sensor and shaft tilt angle was calculated [7]. Optical method could attain high precision. However, a rotating shaft large enough was needed so that the reflector could be installed, and the shaft had to be located outside for

light projection. Tanachaikhan measured the shaft tilt angle by recording the magnetic flux density. Its resolution of shaft rotation was 1 degree per step and its range of shaft decline varied from 4° to 10° [8]. This method is novel, but does not meet the accuracy requirement (<10 arc sec) of some measurement instruments. Therefore, these methods are not practical in a large number of applications, such as three dimensional profile rotary measuring system and north-finder.

Unlike a conventional measurement system, a dual-axis inclinometer is applied to measure the rotating shaft tilt angle instead of plane angle in this paper. The relationship between the rotating shaft tilt angle and inclinometer outputs is extensively analyzed. The precision and resolution of the inclinometer we used are $\pm 0.01^\circ$ and 0.0005° , respectively. Experiment results showed measurement standard deviation of the rotating shaft tilt angle was 0.0006° and the range was 0.0018° .

In this paper, section 1 reviews different methods to measure the rotating shaft tilt angle. Section 2 introduces our mechanical structure and develops the principle of using a dual-axis inclinometer to measure rotating shaft tilt angle under the condition that the rotating shaft is perpendicular to the inclinometer axes. In section 3, we illustrate how to use reversal measurement method to attain high precision in practical measurement environment, *i.e.* the inclinometer axes are not perpendicular to the rotating shaft. Section 4 estimates the measurement uncertainty of the system. In section 5, several experiments were implemented to verify the proposed method. Finally, conclusions are presented in section 6.

2. MEASUREMENT MODEL

An inclinometer is an instrument for measuring angles of slope, elevation of an object with respect to gravity and it generates an artificial horizon and measures angular tilt with

respect to this horizon, which is extensively applied in a large number of applications, such as robot control, or attitude navigation system. Therefore, researchers use it to measure the tilt angle of a plane, rather than a shaft [9 - 11].

In this part, the principle of using a dual-axis inclinometer to measure a rotating shaft tilt angle is developed. The mechanical structure model, as shown in Fig.1., is designed to measure the rotating shaft tilt angle. It consists of a dual-axis inclinometer, a platform, a rotating shaft, a torque motor, an encoder, and a supporting frame. The inclinometer is mounted on the surface of the platform which is fixed on the rotating shaft. X+ and Y+ axes on the inclinometer illustrate the directions and polarities of the two orthogonal tilt directions. A downward rotation of the X+ arrowhead produces a negative tilt angle in inclinometer X+ axis output, and an upward rotation of the X+ arrowhead produces a positive tilt angle in inclinometer X+ axis output, similarly, the same rules apply to Y+ axis. The torque rotates the rotating shaft, alongside the platform and the inclinometer. The encoder records the rotation angle of the rotating shaft.

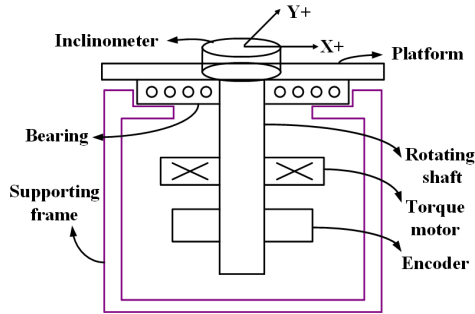


Fig.1. Rotating shaft tilt angle measurement mechanical structure.

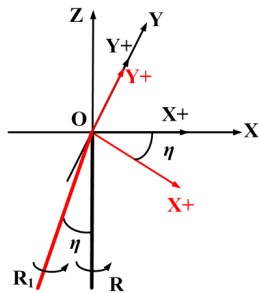


Fig.2. Using an inclinometer to measure rotating shaft tilt angle.

We assume the inclinometer, the platform and the shaft are mounted ideally, which means the inclinometer X+ and Y+ axes are perpendicular to the rotating shaft. Based on the mechanical structure in Fig.1., the shaft tilt angle measurement model is developed, as shown in Fig.2. Point O is the center of the inclinometer, OXYZ is the Cartesian world coordinate system, and OXY is parallel to the horizontal plane. OR represents the rotating shaft in vertical state and OR₁ indicates the rotating shaft in tilt state. OR₁ is obtained by rotating OR clockwise η along the Y axis. η , the angle between the shaft in vertical state and the shaft in tilt state, is defined as the rotating shaft tilt angle. Two important properties of the rotating shaft should be noted.

Firstly, the tilt angle η is fixed when we rotate the shaft around its own axis. Secondly, if the rotating shaft is perpendicular to the horizontal plane, the inclinometer outputs in X+ and Y+ axes do not change when the shaft is rotated.

When $\eta \neq 0$, the red X+ axis does not coincide with the black X+ one; the angle between them equals to η . If OR₁ is rotated counterclockwise around its own axis, both of the red X+ axis output and red Y+ axis output shall change as the shaft rotates.

The shaft tilt angle η is calculated according to inclinometer outputs and the relationship between the rotating shaft and the inclinometer. To calculate it, three cases need to be considered according to the outputs of X+ axis and Y+ axis, as shown in Fig.3., Fig.4. and Fig.5.

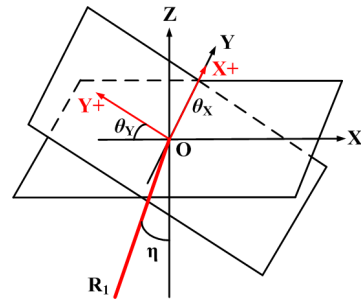


Fig.3. Case 1: $\theta_X=0$ and $\theta_Y \neq 0$.

Let us make γ the counterclockwise rotation angle of rotating shaft OR₁ around its own axis. In Fig.2., $\gamma=0^\circ$, and it equals 90° in Fig.3. θ_X denotes the inclinometer output of the X+ axis, and θ_Y denotes that of the Y+ axis. In Fig.3., $\theta_X=0$ because the X+ axis is parallel to X axis (horizontal plane), and $\theta_Y \neq 0$ because the Y+ axis is not parallel to Y axis.

As shown in Fig.3., the tilted plane is the plane X+Y+. (x, y, z) represents a point in the coordinate system XYZ. The equation of plane X+Y+ is $z=0$ when $\eta=0^\circ$; it is $\sin(\eta) \cdot x + \cos(\eta) \cdot z=0$ when $\eta \neq 0^\circ$. Therefore, in this case, $\eta=\theta_Y$.

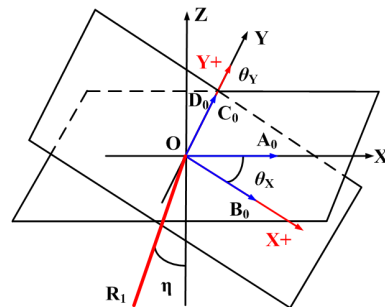


Fig.4. Case 2: $\theta_X \neq 0$ and $\theta_Y=0$.

Fig.4. is obtained when $\gamma = 0^\circ$. In this case, $\theta_X \neq 0$ and $\theta_Y=0$, $\eta=\theta_X$. In order to calculate η in case 3, some vectors are defined in Fig.4. Vector $\mathbf{OA}_0=(1,0,0)$ in X direction is in the $z=0$ plane, and its projection to the $\sin(\eta) \cdot x + \cos(\eta) \cdot z=0$ plane is vector $\mathbf{OB}_0=(\cos\eta, 0, -\sin\eta)$. Vector $\mathbf{OC}_0=(0,1,0)$ in Y direction is in the $z=0$ plane, and vector $\mathbf{OD}_0=(0,1,0)$ is its projection to the $\sin\eta \cdot x + \cos\eta \cdot z=0$ plane.

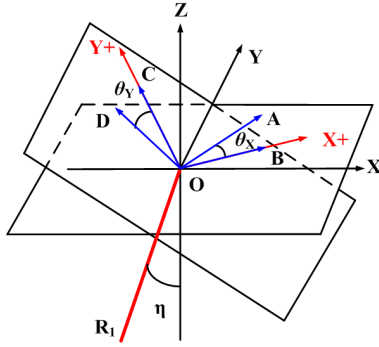

 Fig.5. Case 3: $\theta_x \neq 0$ and $\theta_y \neq 0$.

Fig.5. illustrates the third case: $\theta_x \neq 0$ and $\theta_y \neq 0$. It is obtained when $\gamma \neq 90^\circ \cdot I$ (I is an integer). Vectors \mathbf{OA}_0 and \mathbf{OB}_0 are rotated at the same angle γ as \mathbf{OR}_1 , and \mathbf{OA}_0 and \mathbf{OB}_0 become vector $\mathbf{OA}=(x_A, y_A, z_A)$ and $\mathbf{OB}=(x_B, y_B, z_B)$, respectively. In the $z=0$ plane,

$$\begin{cases} x_A^2 + y_A^2 + z_A^2 = 1 \\ z_A = 0 \\ \cos \gamma = x_A \end{cases} \quad (1)$$

In the $\sin(\eta) \cdot x + \cos(\eta) \cdot z = 0$ plane,

$$\begin{cases} x_B^2 + y_B^2 + z_B^2 = 1 \\ \sin(\eta) \cdot x_B + \cos(\eta) \cdot z_B = 0 \\ \cos \gamma = \cos(\eta) \cdot x_B - \sin(\eta) \cdot z_B \end{cases} \quad (2)$$

Point $A = (\cos \gamma, \sin \gamma, 0)$ and $B = (\cos \eta \cos \gamma, \sin \eta \cos \gamma, -\sin \eta \sin \gamma)$ are calculated based on (1) and (2). $\angle AOB$ is equal to θ_x according to the inclinometer angle measurement principle, then

$$\cos \theta_x = \cos \eta \cos \gamma^2 + \sin \gamma^2 \quad (3)$$

Vector \mathbf{OC}_0 and \mathbf{OD}_0 are rotated angle γ too, and \mathbf{OC}_0 and \mathbf{OD}_0 become $\mathbf{OC}=(x_C, y_C, z_C)$ and $\mathbf{OD}=(x_D, y_D, z_D)$, respectively. In the $z=0$ plane,

$$\begin{cases} x_C^2 + y_C^2 + z_C^2 = 1 \\ z_C = 0 \\ \cos \gamma = y_C \end{cases} \quad (4)$$

In the $\sin(\eta) \cdot x + \cos(\eta) \cdot z = 0$ plane,

$$\begin{cases} x_D^2 + y_D^2 + z_D^2 = 1 \\ \sin(\eta) \cdot x_D + \cos(\eta) \cdot z_D = 0 \\ \cos \gamma = y_D \end{cases} \quad (5)$$

According to (4) and (5), point $C=(-\sin \gamma, \cos \gamma, 0)$, $D=(-\cos \eta \sin \gamma, \cos \gamma, \sin \eta \sin \gamma)$ are achieved. $\angle COD$ is equal to θ_y according to inclinometer property, then

$$\cos \theta_y = \cos \eta \sin \gamma^2 + \cos \gamma^2 \quad (6)$$

According to (3) and (6),

$$\eta = \arccos(\cos \theta_x + \cos \theta_y - 1) \quad (7)$$

Equation (7) combines η , θ_x and θ_y together, and η is calculated by measuring the inclinometer outputs. It also explains the first case and second case: η is equal to θ_x or θ_y if one of the inclinometer outputs is zero. However, there exist three factors which restrain the above method to attain high tilt angle measurement precision. The first factor is that the inclinometer is connected to the shaft via the platform, so the angles between the rotating shaft and inclinometer axes do not equal 90° because of manufacture or installation error. The second factor is that the inclinometer is sensitive to temperature, so its output angle could be greater or smaller than the actual angle when the temperature fluctuates [12]. Using this method, the inclinometer has to be calibrated properly because of manufacturing defects, like misalignment of the inertial sensor axes during construction, soldering, or packaging [13].

3. REVERSAL MEASUREMENT

Section 2 explains how to measure the tilt angle when the inclinometer axes are perpendicular to the rotating shaft. This section focuses on calculating the angle in real applications, regardless whether the inclinometer axes are vertical to the rotating shaft or not. Reversal measurement [14] is a well-known method that eliminates the inclinometer systematic error. To achieve high accuracy, we propose a rotating shaft tilt angle reversal measurement method that solves several problems, including inclinometer systematic error, inclinometer zero offset and sensitivity to temperature fluctuation, and mechanical errors (manufacture deflection of rotating shaft, the inclinometer and the platform; installation deviation among the above parts).

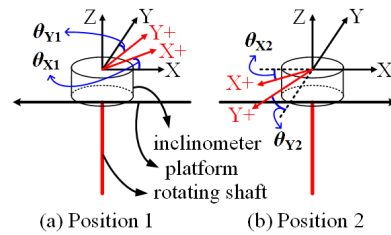


Fig.6. The proposed reversal measurement method.

Fig.6. illustrates the two measurement procedures in practical situation. The Cartesian coordinate system $OXYZ$ is built according to the position of $X+$ axis and $Y+$ axis, guaranteeing that $X+$ axis is in the OXZ plane and $Y+$ axis is in the OYZ plane when the inclinometer is in position 1 or position 2. Our measurement procedure includes two steps. First, the inclinometer axes outputs are obtained at position 1 (Fig.6.a)), and θ_{x1} , θ_{y1} indicate $X+$ axis and $Y+$ axis outputs, respectively. Then, rotate the rotating shaft by γ , that is 180° , to position 2 (Fig.6.b)). θ_{x2} , θ_{y2} indicate $X+$ axis and $Y+$ axis outputs, respectively.

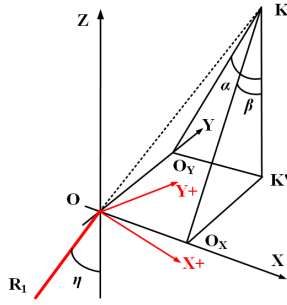
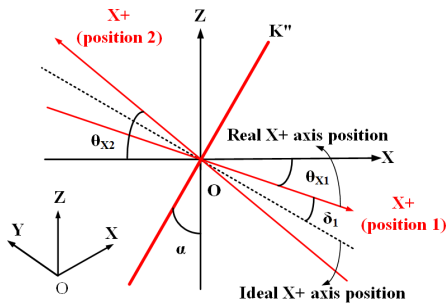


Fig. 7. Projection of rotating shaft tilt angle.

It is noted that in Fig. 5. we assume OR_1 is in OXZ plane, and $X+$ axis or $Y+$ axis is not located in a fixed plane. However, in real applications (reversal measurement), the position of rotating shaft OR_1 is not in a fixed plane; it can be located in OXZ plane, OYZ plane or in the space between the two planes. Fig. 7. shows the last situation, which is OR_1 located in the space between plane OXZ and plane OYZ .

Let us extend OR_1 , and K is a point on the extension line. The projection of point K on plane OXY is denoted as K' . Point O_X and O_Y are the projection of point K' on the X axis and Y axis, respectively. Therefore, plane $O_YK K'$ is parallel to plane OXZ , and plane $O_XK K'$ is parallel to plane OYZ . We denote the $\angle O_YK K'$ as α , and $\angle O_XK K'$ as β . Angle α equals to the angle between the Z axis and the projection of OR_1 on plane OXZ . Similarly, angle β is equivalent to the angle between the Z axis and the projection of OR_1 on plane OYZ .

Let us see the OXZ plane in Fig. 7., as shown in Fig. 8. OK'' in Fig. 8. is parallel to O_YK in Fig. 7. The dash line, representing the ideal $X+$ axis, is perpendicular to OK'' .


 Fig. 8. Calculate the rotating shaft tilt angle (projection angle) α using the reversal measurement method.

θ_{X1} and θ_{X2} are the inclinometer outputs along the $X+$ axis at position 1 and position 2, respectively. In real applications, the real $X+$ axis is not perpendicular to the rotating shaft. There exists a small angle δ_1 between the real $X+$ axis and the ideal one. Here, δ_1 represents mechanical errors, such as manufacture deflection of rotating shaft, the inclinometer and the platform; installation deviation among all of them. Comparing Fig. 5. with Fig. 8., it is clear that θ_X is equal to α in Fig. 8. In Fig. 5., θ_X is the angle between the ideal $X+$ axis and the horizontal plane. In Fig. 8., α equals $\theta_{X1} + \delta_1$, that is to say, α equals to the angle θ_X .

The physical significance of inclinometer $X+$ axis output is: a downward (upward) rotation of the $X+$ arrowhead produces a negative (positive) output in $X+$ axis. In Fig. 8., θ_{X1} is negative, and θ_{X2} is positive. In order to calculate α , the sign rules of δ_1 , α and $\theta_{X1}(\theta_{X2})$ are defined in Table 1.

 Table 1. The sign rules of δ_1 , α , $\theta_{X1}(\theta_{X2})$.

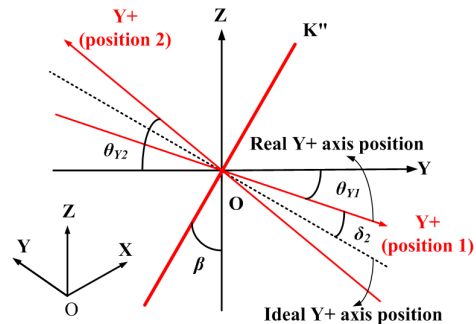
| sign | rule |
|--------------------------------|--|
| $\delta_1 > 0$ | Ideal $X+$ is higher than real $X+$ |
| $\delta_1 = 0$ | Ideal $X+$ is parallel to real $X+$ |
| $\delta_1 < 0$ | Ideal $X+$ is lower than real $X+$ |
| $\alpha > 0$ | OK'' rotates clockwise along Y axis |
| $\alpha = 0$ | OK'' is parallel to Z axis |
| $\alpha < 0$ | OK'' rotates counterclockwise along Y axis |
| $\theta_{X1}(\theta_{X2}) > 0$ | real $X+$ is higher than the horizontal plane |
| $\theta_{X1}(\theta_{X2}) = 0$ | real $X+$ is parallel to the horizontal plane |
| $\theta_{X1}(\theta_{X2}) < 0$ | real $X+$ is lower than the horizontal plane |

According to the sign rules in Table 1 and geometrical relationship in Fig. 8.,

$$\begin{cases} \theta_{X2} = -\theta_{X1} - 2\delta_1 \\ \alpha = -\theta_{X1} - \delta_1 \end{cases} \quad (8)$$

$$\alpha = \frac{\theta_{X2} - \theta_{X1}}{2} = \theta_X \quad (9)$$

Fig. 9. shows the OYZ plane in Fig. 7. OK'' in Fig. 9. is parallel to O_XK in Fig. 7. The dash line, representing the ideal $Y+$ axis, is perpendicular to OK'' . θ_{Y1} and θ_{Y2} are the inclinometer outputs along the $Y+$ axis at position 1 and position 2, respectively. δ_2 represents the small angle between the real $Y+$ axis and the ideal one. β in Fig. 9. equals to θ_Y in Fig. 5. because both represent the angle between the ideal $Y+$ axis and horizontal plane. The sign of δ_2 , β and θ_{Y1} (θ_{Y2}) follow the similar sign rules with δ_1 , α and $\theta_{X1}(\theta_{X2})$, respectively. Based on the sign rules and Fig. 9., (10) and (11) are obtained,


 Fig. 9. Calculate the projection angle β using the reversal measurement method.

$$\begin{cases} \theta_{Y2} = -\theta_{Y1} - 2\delta_2 \\ \beta = -\theta_{Y1} - \delta_2 \end{cases} \quad (10)$$

$$\beta = \frac{\theta_{Y2} - \theta_{Y1}}{2} = \theta_Y \quad (11)$$

Based on (7), η is accurate if θ_X and θ_Y are measured accurately. In our method, θ_X and θ_Y are calculated by reversal measurement to achieve high accuracy. Let us have a look on (9) and (11). Firstly, the outcome of θ_X (α) and θ_Y (β) does not include δ_1 and δ_2 , so the mechanical errors are eliminated. Secondly, the inclinometer systematic error is eliminated by subtracting the inclinometer outputs in position 1 from position 2. Finally, the zero offset and sensitivity of the inclinometer are largely decreased by subtracting the inclinometer outputs in position 1 from position 2 because the measurement is conducted in a short time. Equation (12) is obtained by substituting (9), (11) into (7),

$$\eta = \arccos\left(\cos\left(\frac{\theta_{X2} - \theta_{X1}}{2}\right) + \cos\left(\frac{\theta_{Y2} - \theta_{Y1}}{2}\right) - 1\right) \quad (12)$$

In real applications, η is calculated based on (12).

4. UNCERTAINTY ESTIMATION

In order to estimate the total uncertainty in a measurement, each critical component must be identified and its uncertainty must be quantified [15]. The primary parameter components in the shaft tilt angle measurement described in this paper include the shaft rotation angle γ which is determined by the encoder, θ_{X1} , θ_{Y1} , θ_{X2} , θ_{Y2} measured by the inclinometer.

In the practical reversal measurement process, the shaft rotation angle cannot be 180° exactly, $\sigma(\theta_{Xi})$ ($i=1,2$), $\sigma(\theta_{Yi})$ denote the uncertainty of θ_{Xi} , θ_{Yi} , and can be expressed as,

$$\begin{cases} \sigma(\theta_{Xi}) = (\partial\theta_{Xi}/\partial\gamma)u_\gamma, i=1,2. \\ \sigma(\theta_{Yi}) = (\partial\theta_{Yi}/\partial\gamma)u_\gamma \end{cases} \quad (13)$$

u_γ is the uncertainty of the rotation angle determined by encoder, $\partial\theta_{Xi}/\partial\gamma$ and $\partial\theta_{Yi}/\partial\gamma$ can be obtained based on (3) and (6), respectively.

u_θ is defined as the uncertainty of inclinometer, and both the inclinometer uncertainty and the shaft rotation error affect the accuracy of η . The total uncertainty of the measurement caused by the inclinometer uncertainty and shaft rotation uncertainty are defined as,

$$\begin{cases} u_{Xtotal}^2 = (u_\theta)^2 + \sigma_{\theta_{Xi}}^2 \\ u_{Ytotal}^2 = (u_\theta)^2 + \sigma_{\theta_{Yi}}^2 \end{cases}, i=1,2. \quad (14)$$

Therefore, the total uncertainty of η is σ_η ,

$$\sigma_\eta^2 = (\partial\eta/\partial\theta_{Xi})^2 (u_{Xtotal})^2 + (\partial\eta/\partial\theta_{Yi})^2 (u_{Ytotal})^2 \quad (15)$$

$\partial\eta/\partial\theta_{Xi}$ and $\partial\eta/\partial\theta_{Yi}$ can be obtained based on (12). Firstly, σ_η analysis is performed by changing the η individually from 0.0001° to 5° , $u_\theta=0.0005^\circ$ (data based on inclinometer specification sheet) and $u_\gamma=0.0125^\circ$ (data based on the

encoder specification sheet) are used to plot Fig.10. based on (15). σ_η is less than $3.55 \times 10^{-4}^\circ$ from 0.0001° to 5° in the simulation. Secondly, we assume η is fixed and $\eta=0.5^\circ$, Fig.11. is plotted by changing u_θ from 0.0001° to 0.01° , and it shows the inclinometer uncertainty has a big influence on σ_η . Therefore, higher inclinometer resolution is required for better rotating shaft tilt angle measurement results.

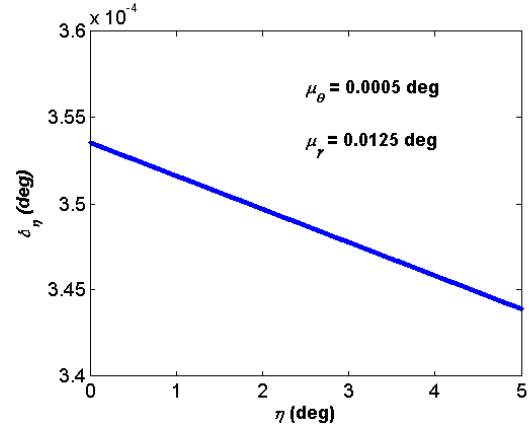


Fig.10. η uncertainty when the rotating shaft tilt ranges from 0.0001 degrees to 5 degrees.

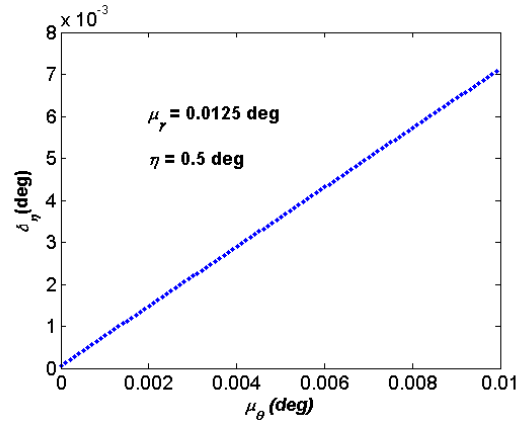


Fig.11. η uncertainty when the inclinometer resolution ranges from 0.0001 degrees to 0.01 degrees.

5. EXPERIMENTS & RESULTS

NS-5/P2 inclinometer was chosen to measure the rotating shaft tilt angle, whose configuration is shown in Table 2. The inclinometer response time is about 0.3 seconds, and inclinometer outputs were obtained every 0.5 seconds in the experiment. The temperature drifts of zero and sensitivity is no more than $5 \times 10^{-4}/^\circ\text{C}$ and $1 \times 10^{-3}/^\circ\text{C}$, respectively. It indicates the inclinometer outputs were stable in short time. However, the output will fluctuate heavily if the inclinometer is exposed to an environment for a long time. PID algorithm was adapted to control the torque motor to ensure fast rotation speed, and a total experiment time of 4 seconds is achieved. The encoder recorded the rotation angle and commanded the torque motor to stop if it detected the difference of setting angle and current angle was less than 0.0125° at positions 1 and 2, which guaranteed the rotation uncertainty was 0.0125° .

Table 2. Configuration of NS-5/P2.

| Description | Value |
|-----------------------------|---|
| Measurement range | $\pm 5^\circ$ |
| Precision(Digital) | $\pm 0.01^\circ$ |
| Resolution | 0.0005° |
| Measurement time | 0.3s |
| Zero point | $< 5 \times 10^{-4}^\circ \text{C}$ |
| Sensitivity | $< 1 \times 10^{-3}^\circ \text{C}$ |
| Operating temperature range | $-25^\circ \text{C} \sim 85^\circ \text{C}$ |
| Output structure | $\pm \text{XX.XXX}, \pm \text{YY.YYY}$ |

5.1. Reversal measurement

Two experiments were conducted to test the effectiveness of the reversal measurement method. The experiment device was put on a steady platform at daytime in the first experiment. The experiment procedure is as follows: move the inclinometer and rotating shaft to position 1 by torque motor and record the outputs θ_{X1} , θ_{Y1} after power on; then rotate them by 180° to position 2 and record θ_{X2} , θ_{Y2} . The experiment procedure was conducted repeatedly every 5 minutes, and the whole experiment lasted 45 minutes. As can be seen from Fig.12., θ_{X1} rises smoothly from 0.397° to 0.464° in 45 minutes at position 1, and θ_{X2} goes up from -0.953° to -0.886° at position 2. At the same time, θ_{Y1} , θ_{Y2} both increase by 0.067° during the measurement time.

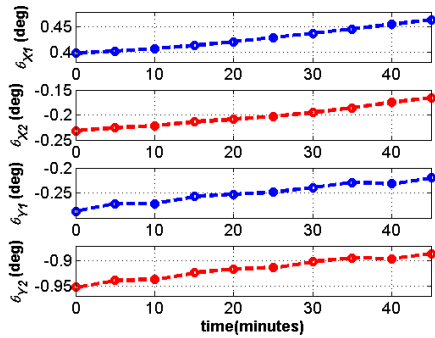
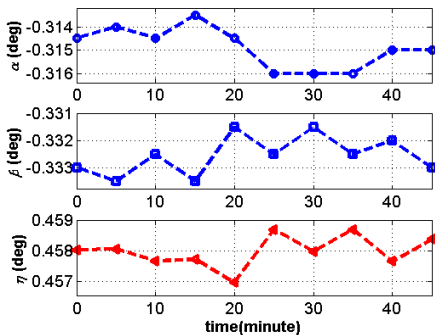
Fig.12. First group data of θ_{X1} , θ_{Y1} , θ_{X2} , θ_{Y2} .

Fig.13. First group data of rotating shaft tilt angle measurement.

Fig.13. shows α , β and η , which is plotted using the data in Fig.12. α and β are stable, and the range of η is 0.0018° .

In the second experiment, spacer was put under the supporting frame to change the rotating shaft tilt angle and was conducted in the evening. Fig.14 is the data of θ_{X1} , θ_{Y1} , θ_{X2} , θ_{Y2} we recorded during 45 minutes after power on. It is clear that θ_{X1} rises from -0.082° to -0.076° , and then drops to -0.088° at position 1. The fluctuation trend of θ_{X2} is almost the same with θ_{X1} ; it grows from 0.397° to 0.4° , and declines to 0.388° in the end at position 2. The general fluctuation trend of θ_{Y1} is similar to θ_{Y2} in 45 minutes.

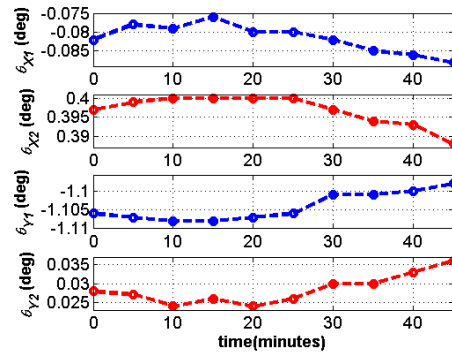
Fig.14. Second group data of θ_{X1} , θ_{Y1} , θ_{X2} , θ_{Y2} .

Fig.15. is plotted to show the fluctuation trend of α , β and η based on Fig.14. Over the period of 45 minutes, the range of η is 0.0018° .

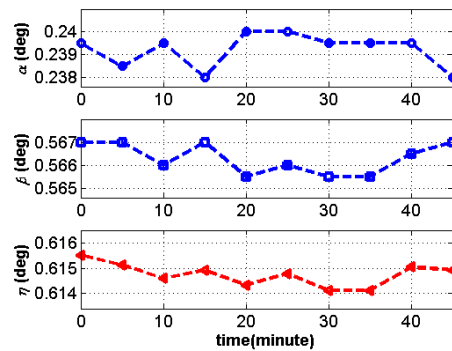


Fig.15. Second group data of rotating shaft tilt angle measurement.

α , β and η stay steady regardless of the inclinometer drifts caused by temperature change in both experiments. Two experiments with standard deviation of θ_{X1} , θ_{X2} , θ_{Y1} , θ_{Y2} , α , β and η are plotted in Fig.16.

In the first experiment, the inclinometer outputs add up to nearly 0.07° in 45 minutes. However, their fluctuation trends at position 1 are almost the same as at position 2, and the standard deviation of θ_{X1} , θ_{X2} , θ_{Y1} , θ_{Y2} is about 0.022° . As a result, the standard deviation of η is $5.4 \times 10^{-4}^\circ$. In the second experiment, although the fluctuation trend of inclinometer outputs in the second experiment is completely different from the first one, the standard deviation of η is $6 \times 10^{-4}^\circ$ and it is nearly equal to the inclinometer resolution.

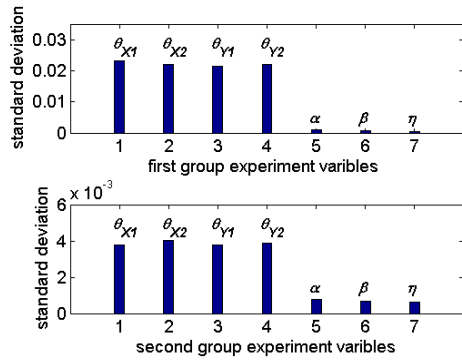


Fig.16. Standard deviation of two groups.

Contrasting the data in Fig.12. and Fig.14., we noticed that the inclinometer outputs rise continuously in the first experiment. However, the fluctuation trend is different in the second experiment, which increases at first then declines after the sixth measurement. The reason leading to this result is that the environment temperature is different in the two group experiments. Although the temperature fluctuation trend is different, these two experiments achieved almost the same accuracy. It illustrates that the proposed method is effective in different temperature environments.

5.2. One circle measurement

In the above experiments, position 1 and position 2 are fixed in each experiment. We executed another experiment to verify that the rotating shaft tilt angle is a fixed value when the shaft is rotated around its own axis. One circle is divided into 36 parts averagely; it means that the first part is position 1 at 0° and position 2 at 180°; the thirty-six part is position 1 at 350° and position 2 at 170°. Then reversal measurement method is applied to measure the rotating shaft tilt angle η at each part. Fig.17. is plotted based on the θ_{x1} , θ_{y1} , θ_{x2} , θ_{y2} we recorded; the red lines are the simulation results according to (3), (6) and (7), the blue ones are experiment points which are calculated according to (10) and (11). It is clear that the deviations of α and β are fairly small and the rotating shaft tilt angle remains stable when torque motor rotates the shaft. The standard deviation of η is $7 \times 10^{-4}^\circ$ and the range of η is 0.0026° , which accords to the theoretical analysis that rotating shaft tilt angle is the same regardless of the rotation angle.

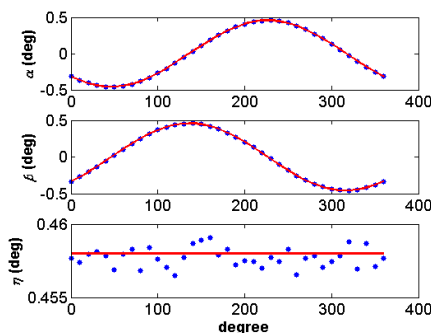


Fig.17. One-circle measurement.

6. CONCLUSION

This paper presents a new method for rotating shaft tilt angle measurement using a dual-axis inclinometer, which is suited for the applications where high accuracy is required. The rotating shaft model is developed according to the north-finder; the reversal measurement method is adapted to eliminate the mechanical error, the inclinometer systematic error, and to decrease the impact of inclinometer drifts. Due to this measurement principle, this method is intrinsically robust and the uncertainty estimation indicates the measurement uncertainty is nearly equal to the inclinometer resolution.

Apart from the inclinometer we use in our experiment, other two-axis inclinometer, such as LCA328T, ACA628T, can be used in our method. Alternatively, our method can also be applied with a one dimensional inclinometer, and two different reversal measurements are required to measure α and β sequentially.

Rotating shaft is widely used in precision machine process and precision instrument. The proposed method only demands an inclinometer and it is easy to execute. The measurement time is a few seconds and has high precision, which could be used for aligning the rotating shaft. Further work can be automatically aligning the tilted shaft based on the tilt angle measured by inclinometer.

ACKNOWLEDGEMENT

The work was supported by the Jilin key scientific and technological projects (20150204013GX). We thank the two anonymous reviewers for their constructive comments.

REFERENCES

- [1] Chen, B., Zhang, X., Zhang, H., He, X., Xu, M. (2014). Investigation of error separation for three dimensional profile rotary measuring system. *Measurement*, 47, 627-632.
- [2] Liu, Z., Zhu, J., Yang, L., Liu, H., Wu, J., Xue, B. (2013). A single-station multi-tasking 3D coordinate measurement method for large-scale metrology based on rotary-laser scanning. *Measurement Science and Technology*, 24 (10), 105004.
- [3] Prihodko, I.P., Zotov, S.A., Trusov, A.A., Shkel, A.M. (2013). What is MEMS gyrocompassing? Comparative analysis of maytagging and carouseling. *Journal of Microelectromechanical Systems*, 22 (6), 1257-1266.
- [4] Mu-Jun, X., Li-Ting, L., Zhi-Qian, W. (2012). Study and application of variable period sampling in strap-down north seeking system. *Energy Procedia*, 16, 2081-2086.
- [5] Arnaudov, R., Angelov, Y. (2005). Earth rotation measurement with micromechanical yaw-rate gyro. *Measurement Science and Technology*, 16 (11), 2300.
- [6] Fang, S., Liu, Y., Wang, H., Taguchi, T., Takeda, R. (2013). Compensation method for the alignment angle error of a gear axis in profile deviation measurement. *Measurement Science and Technology*, 24 (5), 055008.
- [7] Li, K., Kuang, C., Liu, X. (2013). Small angular displacement measurement based on an autocollimator and a common-path compensation principle. *Review of Scientific Instruments*, 84 (1), 015108.

- [8] Tanachaikhan, L., Tammarugwattana, N., Sriratana, W., Klongratog, P. (2009). Declined angle analysis of shaft using magnetic field measurement. In *ICCAS-SICE*, 18-21 August 2009. IEEE, 1846-1849.
- [9] Yang, W., Fang, B., Tang, Y.Y., Qian, J., Qin, X., Yao, W. (2013). A robust inclinometer system with accurate calibration of tilt and azimuth angles. *IEEE Sensors Journal*, 13 (6), 2313-2321.
- [10] Liu, Y., Fang, S., Otsubo, H., Sumida, T. (2013). Simulation and research on the automatic leveling of a precision stage. *Computer-Aided Design*, 45 (3), 717-722.
- [11] Kume, T., Satoh, M., Suwada, T., Furukawa, K., Okuyama, E. (2015). Straightness evaluation using inclinometers with a pair of offset bars. *Precision Engineering*, 39, 173-178.
- [12] Zhao, S., Li, Y., Zhang, E., Huang, P., Wei, H. (2014). Note: Differential amplified high-resolution tilt angle measurement system. *Review of Scientific Instruments*, 85 (9), 096104.
- [13] Zhang, Y., Liu, W., Yang, X., Xing, S. (2015). Hidden Markov model - based pedestrian navigation system using MEMS inertial sensors. *Measurement Science Review*, 15 (1), 35-43.
- [14] Kume, T., Satoh, M., Suwada, T., Furukawa, K., Okuyama, E. (2013). Large-scale accelerator alignment using an inclinometer. *Precision Engineering*, 37 (4), 825-830.
- [15] Štubňa, I., Šín, P., Trník, A., Vozár, L. (2014). Measuring the flexural strength of ceramics at elevated temperatures – an uncertainty analysis. *Measurement Science Review*, 14 (1), 35-40.

Received March 23, 2015.

Accepted September 30, 2015.